

Perspective

Steady-State Synthesis of Colloidal Metal Nanocrystals

Jianlong He^{1,†}, Hansong Yu^{2,†}, and Younan Xia^{1,3,*}¹ School of Chemistry and Biochemistry, Georgia Institute of Technology, Atlanta, GA 30332, USA² School of Materials Science and Engineering, Georgia Institute of Technology, Atlanta, GA 30332, USA³ The Wallace H. Coulter Department of Biomedical Engineering, Georgia Institute of Technology and Emory University, Atlanta, GA 30332, USA

* Correspondence: younan.xia@bme.gatech.edu

† These authors contributed equally to this work.

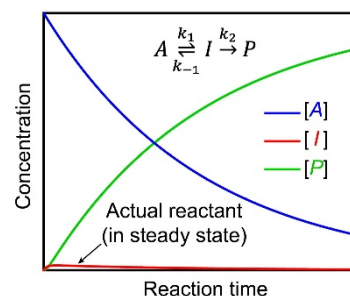
Received: 19 March 2025; Revised: 21 April 2025; Accepted: 25 April 2025; Published: 20 June 2025

Abstract: Despite remarkable progress, colloidal synthesis of metal nanocrystal is still far away from reaching the goal for robust, reproducible, and scalable production. Even with the adoption of seed-mediated growth, the synthesis can still be complicated by issues such as self-nucleation, galvanic replacement, stochastic symmetry reduction, and unwanted compositional variation. All these issues can be addressed by switching to steady-state synthesis characterized by a slow, constant, and tightly controlled reduction rate. Steady-state synthesis can be achieved by adding one reactant dropwise while using the other reactant in large excess, but this method is not suitable for scale-up production in a continuous flow reactor. There is a pressing need to develop alternative methods capable of establishing the steady-state kinetics characteristic of dropwise addition while introducing both reactants by one-shot injection. In this Perspective, we discuss a number of methods that allow for both one-shot injection and steady-state synthesis.

One-shot injection



Growth solution



Reaction time

Keywords: metal nanocrystals; colloidal synthesis; steady-state kinetics; one-shot injection; scalable production

1. Introduction

The last two decades have witnessed the development of many methods capable of producing colloidal metal nanocrystals with uniform sizes and diverse shapes [1–4]. These nanocrystals not only provide a well-defined system to investigate the structure-property relationship [5–7], but also offer opportunities for applications in catalysis, plasmonics, electronics, and medicine [8–14]. Owing to their well-defined surface structures, in particular, these nanocrystals are causing a paradigm shift in an array of catalytic applications for energy conversion (as exemplified by fuel cells and water splitting devices), environmental protection, as well as production of chemicals, pharmaceuticals, and agrochemicals [15–20]. As an immediate advantage over the conventional catalysts based upon poorly-defined nanoparticles, these nanocrystals offer a viable platform to optimize their catalytic performance by maximizing the proportion of the most active and/or selective facets on the surface. For example, the area-specific activities of Pt and Pt₃Ni alloy toward oxygen reduction were enhanced by two and nine folds, respectively, by switching from cubic to octahedral nanocrystals to maximize the proportion of {111} facets on the surface [21–23]. In the case of benzene hydrogenation, only cyclohexene was formed on Pt nanocubes encased by {100} facets while both cyclohexane and cyclohexene were produced on Pt cuboctahedral nanocrystals covered by a mix of {111} and {100} facets [7]. These and many other examples demonstrate the promise held by shape control in augmenting the merits of metal nanocrystals for a spectrum of catalytic applications, both existing and emerging.

Despite recent progress, shape-controlled synthesis of metal nanocrystals is yet to reach the ultimate goal for robust, reproducible, and scalable production. Even with the adoption of seed-mediated growth [24], the products can still become out of control due to the involvement of self-nucleation and/or stochastic symmetry reduction. Recent studies suggest that these issues can be addressed by achieving and keeping the reduction kinetics in a steady state characterized by a constant and relatively slow reduction rate [25,26]. In this case, self-nucleation can



Copyright: © 2025 by the authors. This is an open access article under the terms and conditions of the Creative Commons Attribution (CC BY) license (<https://creativecommons.org/licenses/by/4.0/>).

Publisher's Note: Scilight stays neutral with regard to jurisdictional claims in published maps and institutional affiliations.

be suppressed by slowing down the reduction kinetics and thus maintaining the atom concentration at a level below the threshold for homogeneous nucleation. A constant reduction rate is also advantageous for tightly controlling heterogeneous nucleation and growth. Under steady-state kinetics, for example, the reduction rate can be tuned to different levels, enabling a tight control over the pattern of symmetry reduction.

Owing to its ability to achieve steady-state kinetics, introducing the reactant solution dropwise rather than in one shot has emerged as a powerful tool for a number of synthetic tasks [27,28]. However, it should be noted that dropwise synthesis is not suitable for high-throughput or scale-up production because of the necessity to continuously add the reactant into a reaction system throughout the synthesis and thus the incompatibility with the setting of a continuous flow reactor [29]. There is a pressing need to develop alternative methods capable of achieving the steady-state kinetics characteristic of dropwise addition while introducing the reactant by one-shot injection. Such methods hold the key to the deterministic, reliable, and scalable production of colloidal metal nanocrystals with controllable shapes and related properties.

Building on the principles of chemical kinetics, this perspective examines the feasibility and underlying mechanism to accomplish steady-state synthesis of colloidal metal nanocrystals while the reactants are introduced in one shot. The essence to achieve steady-state kinetics is to keep one of the reactants (e.g., the metal ion) at a stable, relatively low level while the other reactant (e.g., the reductant) is used in large excess so its concentration will stay at the same level during the entire synthesis. Specifically, we discuss the use of consecutive reactions to help maintain the reactant of interest at a stable, relatively low level by balancing the rates for its formation and consumption. Typical examples include (i) the use of ascorbic acid (or another weak acid) as a reductant, with its dissociated form (i.e., the actual reductant) existing in an equilibrium with the acid directly added into a synthesis; (ii) the use of an insoluble salt, with the metal ions (to be reduced to atoms) existing in an equilibrium with the powder added into a synthesis; (iii) the use of an unreactive metal complex, with the metal ions (to be reduced to atoms) existing in an equilibrium with the complex directly added into a synthesis; and (iv) the use of a controlled-release system, where the metal ion or reductant is slowly released and immediately consumed to keep its concentration in a steady state. It is hoped this perspective can serve as a framework for guiding the future synthesis of colloidal metal nanocrystals under steady-state kinetics by providing both practical strategies and mechanistic rationale for their stable and scalable production.

2. Conventional Synthesis Involving One-Shot Injection

For a colloidal synthesis of metal nanocrystals, the reaction kinetics is governed by the second-order rate law because of the requirement for electron transfer and thus collision between the metal ion (M^{m+}) and reductant molecules [30,31]. As such, the reduction rate is directly proportional to the concentrations of both the metal ion and reductant, and it is expected to decay over time as both reactants are continually consumed. As a common practice, one of the two reactants is often used in large excess relative to the other one, so its concentration remains largely fixed during the synthesis. If the reductant is used in large excess, for example, the reduction kinetics can be approximated to follow the pseudo-first-order rate law with regard to the metal ion [32]:

$$R = -d[M^{m+}]/dt = k \cdot [M^{m+}], \quad (1)$$

where k is the rate constant, whose magnitude depends on the coordination ligand binding to the metal ion, the type and concentration of the reductant, as well as the number of active sites on the surface of the growing nanocrystals (or preformed seeds added into the reaction mixture). Upon integration, we obtain:

$$[M^{m+}] = [M^{m+}]_0 \cdot e^{-kt}, \quad (2)$$

with $[M^{m+}]_0$ being the initial concentration of the metal ion. The instantaneous reduction rate can be written as:

$$R = k [M^{m+}]_0 \cdot e^{-kt}. \quad (3)$$

In a conventional synthesis, the metal ion is introduced through one-shot injection. As shown in Figure 1a, its concentration (Equation (2)) and thus the reduction rate (Equation (3)) will both undergo exponential decay as a function of time. For the scenario shown in Figure 1b, it involves a reduction rate constant of $k = 0.5 \text{ min}^{-1}$. Upon injection in one shot, the concentration of the metal ion rapidly rises to 1 M, followed by an exponential decay. The half-life of this pseudo first-order reaction can be calculated as $t_{1/2} = (\ln 2)/k = 1.4 \text{ min}$, indicating that half of the added metal ions will be consumed after only 1.4 min into the synthesis. The reaction will be nearly completed by $t = 10 \text{ min}$ as the concentration of the metal ion is approaching zero, transitioning from exponential decay to steady-state kinetics toward the end of the synthesis. Despite the establishment of a steady state toward the end of a synthesis, there is almost no growth for the nanocrystals as all the added metal ions have been consumed.

The nonlinearity of the reduction rate, as well as its strong dependence on the value of k , has a major impact on the shape and size distribution of the resultant nanocrystals and it can also cause variations to the spatial distributions of different elements in a bi- or multi-metallic system [33]. For example, when synthesizing bimetallic alloy nanocrystals from two distinct metal salts using one-shot injection, the composition of the nanocrystals is expected to vary continuously along the growth direction, as determined by the ratio between the instantaneous reduction rates of the metal salts. At the current stage of development, it remains a challenge to control the compositions of nanocrystals comprised of two or more metals. The issues noted above can be addressed by conducting the synthesis under steady-state kinetics, in which both the metal ion and reductant are maintained at constant concentrations throughout the synthesis.

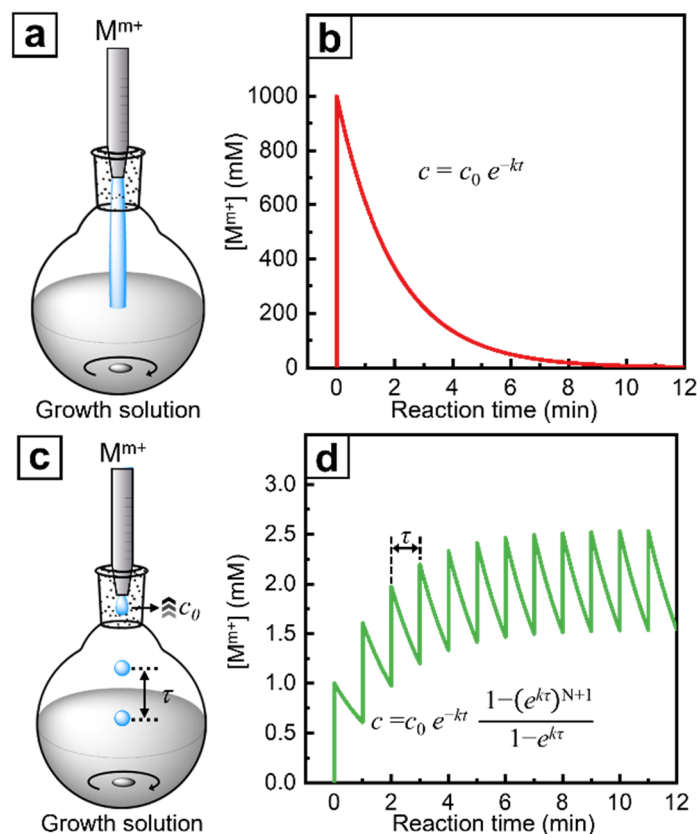


Figure 1. (a,b) Schematic of a synthesis involving one-shot injection of the metal ion and plot of its concentration as a function of time ($c_0 = 1$ M and $k = 0.5$ min⁻¹). (c,d) Schematic of a synthesis involving dropwise addition of the metal ion and plot of its concentration as a function of time ($c_0 = 1$ mM, $k = 0.5$ min⁻¹, and $\tau = 1$ min). Note that the concentrations of the metal ion (the vertical axis), and thus the reduction rates, differ by 2–3 orders of magnitude between these two scenarios. Modified from Ref. [28] with permission.

3. Steady-State Synthesis under Dropwise Addition

One can achieve steady-state kinetics while maintaining growth by switching from one-shot injection to dropwise addition for either the metal ion or the reductant. For example, by adding a solution of the metal ion as regularly-paced droplets into a mixture containing an excess amount of the reductant (Figure 1c), it is practical to maintain the metal ion at a relatively low and stable concentration for the establishment of steady-state kinetics [26]. To simplify the analysis, we assume the solution of the metal ion is added in the form of uniform droplets at a regular pace while neglecting the slight increase in reaction volume when a droplet is introduced. As such, the reduction of the metal ion from individual droplets can be treated as independent events, with the concentration following the same exponential decay as observed in the case of one-shot injection. The addition of the first droplet contributes to a rapid increase in concentration, followed by an exponential decay, as described by Equation (2), until the second droplet arrives. The introduction of each subsequent droplet will induce a similar pattern featuring a sudden increase and then exponential decay in concentration for the metal ion. After six droplets, the concentration of the metal ion in the reaction mixture will enter a steady state. Mathematically, the concentration of the metal ion at time point t can be calculated as the sum of contributions from all the droplets added up to this point [26]:

$$c_t = c_0 \cdot e^{-kt} + c_0 \cdot e^{-k(t-\tau)} + c_0 \cdot e^{-k(t-2\tau)} + \dots + c_0 \cdot e^{-k(t-N\tau)} = c_0 \cdot e^{-kt} (1 - e^{Nk\tau + k\tau}) / (1 - e^{k\tau}), \quad (4)$$

where c_0 is the increase in concentration caused by one droplet of the metal ion solution; τ is the interval of time between adjacent droplets; and N (i.e., t/τ) is the total number of elapsed time intervals. According to Equation (4), c_t is determined by c_0 , k , and τ , and can be calculated for any combination of c_0 and τ if k is known.

As the concentration of the metal ion continually increases, its rate of reduction also increases proportionally. This eventually leads to a steady state in which the decrease in concentration caused by reduction between two adjacent droplets is fully compensated by the increase in concentration contributed by the addition of one droplet. In the steady state, the concentration of the metal ion and thereby the reduction rate only fluctuates between two close values defined by the upper limit (c_{up}) and lower limit (c_{low}). The condition for establishing such a steady state is:

$$c_0 = c_{up} - c_{up} \cdot e^{-k\tau} = c_{up} (1 - e^{-k\tau}). \quad (5)$$

From Equation (5), we have the upper limit as:

$$c_{up} = c_0 / (1 - e^{-k\tau}), \quad (6)$$

and the lower limit as:

$$c_{low} = c_{up} \cdot e^{-k\tau} = c_0 \cdot e^{-k\tau} / (1 - e^{-k\tau}). \quad (7)$$

The average concentration (c_{avg}) in the steady state can be calculated as the total area under the decay curve between two adjacent droplets divided by the duration of time (τ):

$$c_{avg} = \int_0^\tau c_{up} \cdot e^{-kt} \cdot dt / \tau = \left\{ \int_0^\tau [c_0 / (1 - e^{-k\tau})] \cdot e^{-kt} \cdot dt \right\} / \tau = c_0 / (k \cdot \tau). \quad (8)$$

When the synthesis described in Figure 1a is switched from one-shot injection to dropwise addition, the same amount of metal ion solution is divided into 1000 droplets and added at a regular pace with $\tau = 1$ min. As shown in Figure 1d, the concentration of the metal ion in the reaction mixture is maintained at a much lower but stable level throughout the synthesis. Upon the addition of the first droplet, the concentration reaches a low peak of 1.0 mM, equivalent to 0.1% of the concentration associated with one-shot injection. Upon adding the sixth droplet, a steady state is established, with a maximum concentration (i.e., c_{up}) of 2.5 mM. Using Equation (8), the average concentration in the steady state is calculated to be 2.0 mM, which is 400 times lower than the maximum concentration involved in one-shot synthesis. It is worth noting that dropwise addition stretches over a much longer period of 16.7 h, with 99.2% of the synthesis occurring under steady-state kinetics. In this case, the nanocrystals continually grow into larger sizes under the steady-state kinetics.

In addition to the elimination of self-nucleation and control of the pattern of symmetry reduction, steady-state kinetics holds the key to maneuvering the elemental distribution of bi- or multi-metallic nanocrystals as the spatial distributions of the elements are governed by the instantaneous reduction rates of the metal ions involved. In the steady state, the average reduction rate (R_{avg}) can be expressed as:

$$R_{avg} = k \cdot c_{avg} = c_0 / \tau. \quad (9)$$

Significantly, R_{avg} is only dependent on c_0 and τ , not k . As a result, the reactivity of the metal ion becomes irrelevant in determining its reduction rate in the steady state. This unique feature of dropwise addition is instrumental in manipulating the composition of a nanocrystal as it allows for a precise control of the elemental ratio by simply adjusting the concentrations and injection frequencies of the metal ions, regardless of their difference in reactivity. This capability offers immediate advantages. For example, when k increases from 0.5 to 1.0 min⁻¹, the range of variation in reaction rate expands from 0.77–1.27 to 0.58–1.58 mM min⁻¹ due to the changes in c_{up} and c_{low} . However, R_{avg} remains at 1.0 mM min⁻¹, implying that the atomic deposition rate stays unaffected despite the increase in reactivity for the metal ion. As such, if the solutions of the two metal ions are prepared with the same concentration and added into the growth solution dropwise at the same frequency, bimetallic nanocrystals with a uniform atomic ratio of 1:1 will be obtained [34].

In a preliminary study, we utilized the dropwise method to successfully synthesize nanocrystals composed of a quaternary alloy [27]. We used four acetylacetonate complexes as the metal ions for Ru, Rh, Pd, and Pt despite their large difference in reactivity. To assist nucleation and control the facets on the alloy nanocrystals, Rh nanocubes were added as the seeds. A mixture of the different complexes was introduced into the reaction system in the form of tiny droplets that contained approximately 2.2 nmol of each metal per droplet. In this way, the reduction rates of the precursors became synchronized after 1 h into the synthesis (Figure 2a), ensuring the formation of quaternary alloy nanocrystals with a homogeneous and well-controlled surface composition (Figure 2b).

In principle, the reductant can also be added dropwise, while the metal ion is supplied in large excess, to achieve steady-state synthesis. Since the metal ion is often more expensive than the reductant, it is more practical to apply dropwise addition to the metal ion rather than the reductant. Despite the ability to create steady-state kinetics, dropwise addition has a set of drawbacks. Firstly, the metal ion must be continuously added into the reaction system, making it impractical to increase the volume of production by switching from a batch to a continuous flow reactor. Secondly, about six droplets must be added before reaching the steady state. During the reduction of these first six droplets, the growth can be forced to take a specific pattern of symmetry reduction because the deposition of atoms from these six droplets on the surface can create high-energy sites to dictate the following pathway for reduction and atom deposition. Thirdly, in the steady state, the concentration of the metal ion still oscillates within a narrow range defined by C_{up} and C_{low} , and both of them are dependent on k , as shown in Equations (6) and (7). In general, one should minimize the value of k in order to reduce the range of fluctuation and thus possible variations to the spatial distributions of elements along the growth direction. Taken together, there is a need to develop one-shot injection methods capable of creating and maintaining steady-state kinetics throughout the synthesis.

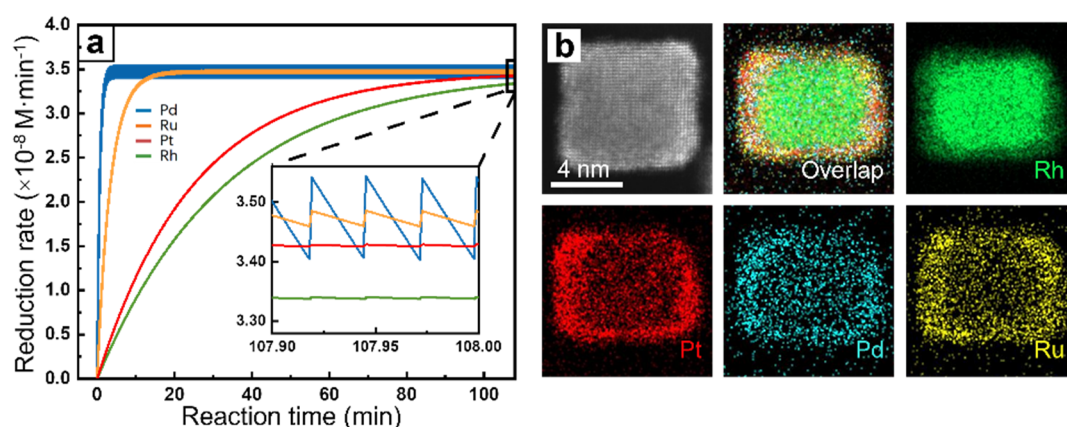


Figure 2. Controlling the composition of quaternary alloy nanocrystals through dropwise addition. (a) Simulated reduction rate as a function of the reaction time in the case of dropwise addition. (b) Scanning transmission electron microscopy image and energy-dispersive X-ray spectroscopy elemental mapping of an alloy nanocrystal, showing the uniform distributions of Rh, Pt, Pd, and Ru. Modified from Ref. [28] with permission.

4. Steady-State Synthesis under One-Shot Injection

An alternative approach to the dropwise method is to avoid directly adding the metal ion or reductant into a synthesis. Instead, a precursor to the metal ion or reductant is used. During a synthesis, the metal ion or reductant will be formed and consumed through consecutive reactions, naturally resulting in the establishment of a steady-state concentration. As an immediate advantage over dropwise addition, the precursor can be added in one shot into the reaction system at the very beginning of a synthesis, making it practical to conduct the colloidal synthesis in a continuous flow reactor.

4.1. Consecutive Reactions Involving an Equilibrium

Let us consider a situation where the metal ion or reductant exists in an equilibrium with the precursor while it is consumed through an irreversible reaction. For simplicity, we can describe this process using the following equation, with reactant A corresponding to the added precursor and intermediate I corresponding to the actual metal ion or reductant involved in the reduction reaction for the generation of product P :



In this case, we can express the reaction rates as:

$$\frac{d[A]}{dt} = -k_1[A] + k_{-1}[I], \quad (11)$$

$$\frac{d[I]}{dt} = k_1[A] - k_{-1}[I] - k_2[I], \quad (12)$$

$$\frac{d[P]}{dt} = k_2[I]. \quad (13)$$

Under the condition of $k_{-1} + k_2 \gg k_1$, a steady state will be achieved, in which the concentration of intermediate I stays at a stable level, with essentially no change over time:

$$\frac{d[I]}{dt} \approx 0. \quad (14)$$

As such, Equation (12) can be rewritten as:

$$\frac{d[I]}{dt} = k_1[A] - k_{-1}[I]_{ss} - k_2[I]_{ss} \approx 0, \quad (15)$$

where $[I]_{ss}$ represents the steady-state concentration of intermediate I . From this equation, $[I]_{ss}$ can be derived as:

$$[I]_{ss} = \frac{k_1}{k_{-1} + k_2} [A]. \quad (16)$$

Meanwhile, Equation (11) can be written as:

$$\frac{d[A]}{dt} = -k_1[A] + k_{-1} \frac{k_1}{k_{-1} + k_2} [A] = -\frac{k_1 k_2}{k_{-1} + k_2} [A]. \quad (17)$$

Upon integration, we have:

$$[A] = [A]_0 e^{-\frac{k_1 k_2}{k_{-1} + k_2} t}. \quad (18)$$

In Figure 3, we plot the concentration profiles of A , I , and P for the case of $A_0 = 100$ mM, $k_2 = 1$, $k_1 = 5k_{-1}$, with the ratios of $k_{-1} + k_2$ to k_1 being 100, 50, 20, 10, 5, and 2, respectively. When the ratio of $k_{-1} + k_2$ to k_1 is greater than 20, the intermediate I can be kept at a stable, relatively low concentration throughout the synthesis, resulting in steady-state kinetics (Figure 3a–c). When the ratio is below 20, as shown in Figure 3d–f, the concentration of I shows a significant increase at the beginning of the synthesis, followed by an exponential decay, like the scenario of a conventional one-shot synthesis.

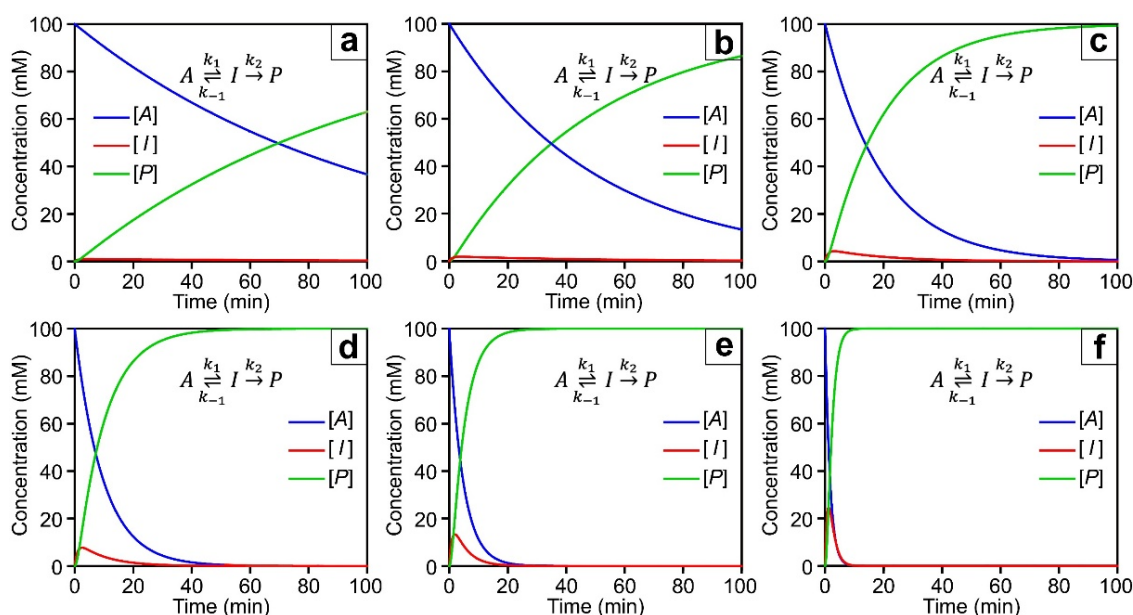


Figure 3. Plots of $[A]$ (blue), $[I]$ (red), and $[P]$ (green) as a function of reaction time in the case of consecutive reactions involving an equilibrium, under the conditions of $A_0 = 100$ mM, $k_2 = 1$, $k_1 = 5k_{-1}$, with the ratios of $k_{-1} + k_2$ to k_1 being (a) 100, (b) 50, (c) 20, (d) 10, (e) 5, and (f) 2.

In practice, reactant A represents the precursor directly added into the reaction system while I pertaining to the actual metal ion or reductant involved in the reduction reaction. In the following sections, we discuss three different approaches that can be explored to achieve steady-state synthesis under one-shot injection by engaging consecutive reactions involving an equilibrium. In these approaches, all the reactants are added in one shot and the establishment of steady-state kinetics can be validated by analyzing the concentration of the metal ion using techniques such as inductively-coupled mass spectrometry (ICP-MS) or UV-vis spectroscopy. As a common

advantage of these approaches, it is feasible to tune the reduction rate in the steady state across a broad range that varies by several orders of magnitude.

4.1.1. Reductant from the Dissociation of a Weak Acid

Carboxylic acids are widely used as reductants in the synthesis of noble-metal nanocrystals [35]. Notable examples include ascorbic acid, citric acid, and formic acid. Upon dissolution in water, the carboxyl group quickly dissociates into carboxylate and proton ions to build an equilibrium:



Typically, A^- would serve as the actual reductant owing to its much stronger reducing power than HA . By simply controlling the pH, it is feasible to maintain the concentration of A^- and thus the reduction rate at constant levels if there is still HA in the reaction solution. Taking ascorbic acid (H_2Asc) as an example, we can write the consecutive reactions as follows:



where DHA represents dehydroascorbic acid. There exists an equilibrium between H_2Asc and $HAsc^-$, while $HAsc^-$ can be subsequently oxidized to DHA by reacting with the metal ion. In a synthesis involving the addition of H_2Asc , $HAsc^-$ serves as the actual reductant to react with the metal ion. Regardless of the concentration of H_2Asc (added into a synthesis in one shot) in the reaction mixture, the concentration of $HAsc^-$ is determined by the dissociation constant (K_a) of H_2Asc and the pH: $[HAsc^-] = K_a/[H^+]$. When the metal ion is used in large excess and thus kept at a stable concentration, one can adjust the concentration of $HAsc^-$ to different levels for the creation of steady states with different reduction rates by simply varying the pH.

In practice, one can also vary the reduction rate constant of ascorbic acid by adjusting the pH. As shown in Figure 4, an aqueous solution of ascorbic acid is dominated by three different species, respectively, when the pH is adjusted from 0–14: acid (H_2Asc), ascorbate ($HAsc^-$), and diascorbate (Asc^{2-}) [35]. For all these forms, the reduction mechanism is similar in terms of electron transfer and the oxidized product, with each molecule donating one pair of electrons for the reduction of a metal ion and the formation of dehydroascorbate as the oxidized product. There is a distinct rate constant associated with each of these forms. As documented in literature, the rate constant (i.e., the reducing power) of ascorbic acid increases as the pH is increased [36–38], primarily due to the involvement of different dominant species. As analyzed above, steady-state kinetics can be achieved for both $HAsc^-$ and Asc^{2-} , but not for H_2Asc . In such a synthesis, it is crucial to control the pH of the reaction mixture, while maintaining the metal ion at a constant concentration, to achieve steady-state kinetics. It is worth noting that most of the synthetic protocols reported in the literature might involve steady-state kinetics albeit this concept has never been explicitly discussed.

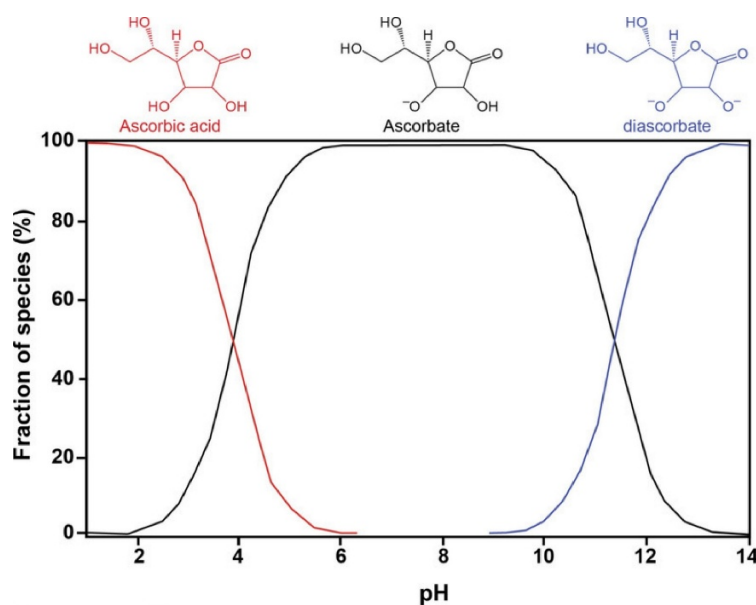


Figure 4. Graph showing the three species derived from ascorbic acid as a function of pH, including H_2Asc at pH below 3, $HAsc^-$ at pH between 6–10, Asc^{2-} at pH above 12. Modified from Ref. [35] with permission.

4.1.2. Metal Ion from the Dissolution of an Insoluble Salt

Insoluble metal salts can also be utilized to achieve steady-state synthesis due to the solubility equilibrium. When the powder of an insoluble salt is added into a reaction solution, it partially dissolves and then dissociates into metal ion and counterion to build an equilibrium:



In this case, the consecutive reactions include the dissolution of the powder and the subsequent reduction of the metal ion, as shown below:



Regardless of the amount of ML_m powder added into the reaction solution, the concentration of the metal ion is only determined by the solubility product constant (K_{sp}) of ML_m and the concentration of the counterion: $[M^{m+}] = K_{sp}/[L^-]^m$. If the reductant is used in large excess relative to the total amount of ML_m , one can adjust the concentration of M^{m+} and thereby attain steady states with different reduction rates by varying the concentration of free L^- in the reaction solution. To this end, powders such as $PdCl_2$, $PdBr_2$, $AgCl$, $AgBr$, and $AuBr_3$ can all be utilized to achieve steady-state synthesis. In general, to achieve the optimal metal ion concentration in the reaction solution, a metal salt with an intermediate dissolution strength is required. It should be neither too strong to be completely soluble, nor too weak so that it can serve as a source of metal ion and maintain a stable M^{m+} concentration in the solution phase. Again, in reviewing the literature, we felt that this concept might have contributed to the success of some protocols without proper discussion. For example, $AgCl$ and $AgBr$ precipitates were often formed in situ during the successful synthesis of some Ag nanocrystals with controlled shapes. The formation of such precipitates might lead to the establishment of steady-state kinetics and thereby enable a tight control over the nucleation and growth. Of course, it should be pointed out that the shape control might also benefit from other mechanisms due to the accelerated photo-reduction of $AgCl$ and $AgBr$ in the presence of Ag seeds. A revisit to, and a systematic study of, such a synthesis is warranted.

4.1.3. Metal Ion from the Dissociation of an Unreactive Complex

Similar to the dissolution of an insoluble salt, steady-state kinetics can also be achieved using an unreactive complex by leveraging its dissociation equilibrium:



when added into the reaction system in one shot, the complex dissociates into the metal ion (the actual precursor) and ligand, followed by reduction of the metal ion:



In this case, the rate constant k_1 (for the dissociation of the complex) should be considerably smaller than the sum of k_{-1} (for the reverse process of dissociation) and k_2 (for the reduction of the metal ion). By choosing an appropriate ligand, it is feasible to control the rate constants k_1 and k_{-1} to ensure $k_{-1} + k_2 \gg k_1$ and thus achievement of steady-state kinetics. For instance, switching from Cl^- to NH_3 , a ligand with a much stronger binding to the Pd^{2+} ion, would allow for the achievement of steady-state synthesis [39].

4.2. Consecutive Reactions Involving No Equilibrium

In some cases, it is also possible to have $k_{-1} = 0$. As such, intermediate I is directly consumed to generate product P without going back to reactant A :



We can define three reaction rates in terms of A , I , P , respectively, as follows:

$$\frac{d[A]}{dt} = -k_1[A], \quad (26)$$

$$\frac{d[I]}{dt} = k_1[A] - k_2[I], \quad (27)$$

$$\frac{d[P]}{dt} = k_2[I]. \quad (28)$$

Integrating $[A]$, $[I]$, $[P]$ with respect to t leads to:

$$[A] = [A]_0 e^{-k_1 t}, \quad (29)$$

$$[I] = \frac{k_1[A]_0}{k_2 - k_1} (e^{-k_1 t} - e^{-k_2 t}), \quad (30)$$

$$[P] = [A]_0 \left[1 + \frac{1}{k_1 - k_2} (k_2 e^{-k_1 t} - k_1 e^{-k_2 t}) \right], \quad (31)$$

In the case of $k_2 \gg k_1$, the concentration of I can be approximated as:

$$[I] \approx \frac{k_1[A]_0}{k_2} (e^{-k_1 t}) = \frac{k_1}{k_2} [A]. \quad (32)$$

In this case, intermediate I will stay at a stable, relatively low concentration, resulting in the establishment of a steady state (I_{ss}). Figure 5 shows the concentration profiles of A , I , and P calculated for the condition of $A_0 = 100$ mM, $k_2 = 1$, with the ratios of k_2 to k_1 being set to 100, 50, 20, 10, 5, and 2, respectively. If the ratio of k_2 to k_1 is greater than 20, intermediate I will stay at a stable, low concentration throughout the reaction, resulting in steady-state kinetics (Figure 5a–c). In contrast, when the ratio of k_2 to k_1 drops below 20, the concentration of intermediate I will show a surge at the beginning, followed by an exponential decay (Figure 5d–f).

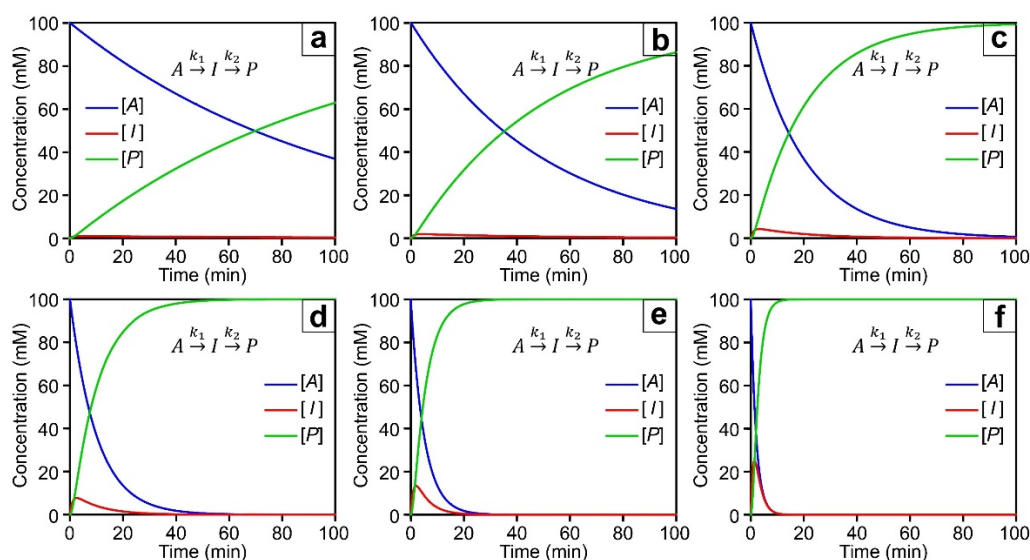


Figure 5. Plots of $[A]$ (blue), $[I]$ (red), and $[P]$ (green) as a function of reaction time in the case of consecutive irreversible reactions, under the conditions of $A_0 = 100$ mM, $k_2 = 1$, and ratios of k_2 to k_1 are (a) 100, (b) 50, (c) 20, (d) 10, (e) 5, and (f) 2, respectively.

Again, there are many good examples of such a synthesis in the literature albeit none of the reports attributed the success to the involvement of steady-state kinetics. Here we choose polyol synthesis as an example to demonstrate the concept. Polyol synthesis has been widely utilized for the production of colloidal noble-metal nanocrystals with controllable shapes [40]. Notable examples include Ag nanowires, nanocubes, and right bipyramids, as well as Au polyhedrons [41–44]. The key feature is the use of a polyol such as ethylene glycol as both the solvent and a precursor to the actual reductant. When heated in air to an elevated temperature, ethylene glycol will be partially oxidized to glycoaldehyde, an intermediate believed to be the reductant responsible for the reduction of metal ion [45]:



This process involves two consecutive reactions: the slow oxidation of ethylene glycol to glycoaldehyde by the oxygen from air and the subsequent fast oxidation of the glycoaldehyde by the metal ion. Under the condition of $k_2 \gg k_1$, glycoaldehyde is expected to exist at a stable, relatively low concentration throughout the synthesis. Although it was not explicitly discussed in the literature, the steady-state kinetics seems to be responsible for the control of both nucleation and growth and thereby the twin structure and shape taken by the nanocrystals. Taking

the synthesis of Ag nanowire as a sample, AgNO₃ can be directly added in one shot into ethylene glycol held at an elevated temperature for the nucleation of decahedral seeds, followed by their growth into penta-twinned Ag nanowires [46–48]. In this process, the Ag⁺ ions from AgNO₃ can be reduced slowly even at a relatively high concentration for the generation of penta-twinned seeds while preventing self-nucleation and unwanted growth.

4.3. Controlled Release of the Reactant from Polymer Beads

In nanomedicine, drugs are often encapsulated in carriers such as polymer beads to achieve zero-order release, by which the drug molecules come out at a constant rate to minimize the fluctuation in plasma concentration while maintaining the plasma drug level in the therapeutic window throughout a treatment, giving the highest therapeutic efficacy [49]. This concept can also be borrowed to achieve steady-state synthesis by pre-loading the metal ion or reductant in polymer beads. As shown in Figure 6, the pre-loaded metal ions undergo a controlled release process from polymer beads into the reaction mixture, followed by reduction into metal atoms. In this process, the slow release of metal ions corresponds to a small release rate constant (k_1), which can be made smaller than the reduction rate constant (k_2), leading to the establishment of steady-state kinetics. In principle, different polymers, such as poly(lactic-co-glycolic acid) of varying compositions can be used to help control the release profile, thereby controlling the magnitude of k_1 [50]. Altogether, it is feasible to maintain the concentration of the metal ion in the reaction mixture at a small and stable by optimizing the release rate constant and/or the reduction rate constant for the establishment of steady states with different rates.

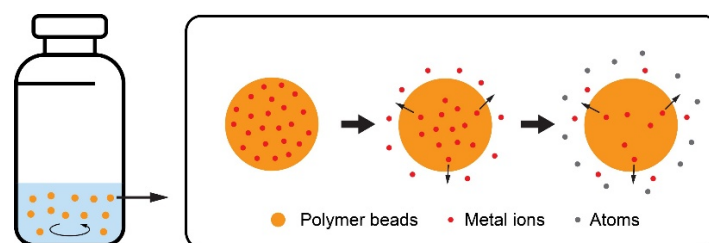


Figure 6. Schematic illustration showing the controlled release of metal ions from polymer beads during a steady-state synthesis of colloidal metal nanocrystals.

5. Concluding Remarks

Achieving robust, reproducible, and scalable production of colloidal metal nanocrystals calls for new methods capable of establishing and maintaining steady-state kinetics in the setting of one-shot injection and continuous flow reactor. The essence is to keep one of the reactants at a stable, relatively low level while the other reactant is used in large excess so the reduction rate will stay at the same level during the entire synthesis. A number of methods are discussed in this Perspective. In the first method, we can leverage the dissociation equilibrium of a weak acid to help maintain the actual reductant at a constant level throughout a synthesis. A notable example is ascorbic acid, whose conjugated bases have much stronger reducing powers than that of the acid. By leveraging the dissociation equilibrium and varying the pH of the reaction solution, we can control the base (the actual reductant) and its concentration at different levels until all the added acid has been consumed. In the second method, we can use an insoluble salt to ensure that the metal ion (the actual precursor) in reaction solution will stay at a constant level controlled by temperature and the concentration of free counterion until all the solid is consumed. In the third method, we can borrow the concept of controlled release from drug delivery by loading the metal ion or reductant in polymer beads. Under zero-order release, the metal ion or reductant in the reaction mixture can be maintained at a low and constant level because it will be immediately consumed as soon as it has been released from the beads. When the other reactant is used in excess, all these methods can be used to achieve steady-state synthesis. In principle, the knowledge gained from the monometallic system can be readily extended to bi- and even multi-metallic systems.

Steady-state synthesis offers immediate advantages over the conventional synthesis that involves reduction rates in an exponential decay. For example, by controlling the reduction rate in the steady state, self-nucleation can be eliminated in the presence of seeds while controlling the pattern of growth, moving toward a reliable, reproducible, and precise synthesis of colloidal nanocrystals. At the moment, steady-state synthesis is mainly achieved through the dropwise addition of the metal salt solution, but this method is not suitable for scale-up production in a continuous flow reactor because of the necessity to continuously add the precursor solution during a synthesis. The methods discussed in this Perspective are capable of achieving steady-state kinetics under one-shot injection, making it practical to directly translate the synthetic method from a batch to a continuous flow

reactor. To our knowledge, all these methods are yet to be explored. They hold the key to the deterministic, reliable, and scalable production of colloidal metal nanocrystals with well-controlled properties.

Author Contributions: Y.X. conceived the concept; J.H. and H.Y. prepared the manuscript and Y.X. revised the writing. All authors have read and agreed to the published version of the manuscript.

Funding: This work was supported in part by research grants from the NSF (CHE-2105602, CBET-2219546, and DMR 2333595), as well as startup funds from the Georgia Institute of Technology.

Data Availability Statement: Not applicable.

Conflicts of Interest: The authors declare no conflict of interest.

References

1. Sun, S.; Murray, C.B.; Weller, D.; Folks, L.; Moser, A. Monodisperse FePt Nanoparticles and Ferromagnetic FePt Nanocrystal Superlattices. *Science* **2000**, *287*, 1989–1992.
2. Jin, R.; Cao, Y.; Mirkin, C.A.; Kelly, K.L.; Schatz, G.C.; Zheng, J.G. Photoinduced Conversion of Silver Nanospheres to Nanoprisms. *Science* **2001**, *294*, 1901–1903.
3. Xia, Y.; Xiong, Y.; Lim, B.; Skrabalak, S.E. Shape-Controlled Synthesis of Metal Nanocrystals: Simple Chemistry Meets Complex Physics? *Angew. Chem. Int. Ed.* **2009**, *48*, 60–103.
4. Nguyen, Q.N.; Wang, C.; Shang, Y.; Janssen, A.; Xia, Y. Colloidal Synthesis of Metal Nanocrystals: From Asymmetrical Growth to Symmetry Breaking. *Chem. Rev.* **2023**, *123*, 3693–3760.
5. Quan, Z.; Wang, Y.; Fang, J. High-Index Faceted Noble Metal Nanocrystals. *Acc. Chem. Res.* **2013**, *46*, 191–202.
6. Sherry, L.J.; Chang, S.-H.; Schatz, G.C.; Van Duyne, R.P.; Wiley, B.J.; Xia, Y. Localized Surface Plasmon Resonance Spectroscopy of Single Silver Nanocubes. *Nano Lett.* **2005**, *5*, 2034–2038.
7. Bratlie, K.M.; Lee, H.; Komvopoulos, K.; Yang, P.; Somorjai, G.A. Platinum Nanoparticle Shape Effects on Benzene Hydrogenation Selectivity. *Nano Lett.* **2007**, *7*, 3097–3101.
8. Guo, S.; Zhang, S.; Sun, S. Tuning Nanoparticle Catalysis for the Oxygen Reduction Reaction. *Angew. Chem. Int. Ed.* **2013**, *52*, 8526–8544.
9. Shi, Y.; Lyu, Z.; Zhao, M.; Chen, R.; Nguyen, Q.N.; Xia, Y. Noble-Metal Nanocrystals with Controlled Shapes for Catalytic and Electrocatalytic Applications. *Chem. Rev.* **2021**, *121*, 649–735.
10. Rathmell, A.R.; Bergin, S.M.; Hua, Y.; Li, Z.; Wiley, B.J. The Growth Mechanism of Copper Nanowires and Their Properties in Flexible, Transparent Conducting Films. *Adv. Mater.* **2010**, *22*, 3558–3563.
11. Li, M.; Zhao, Z.; Cheng, T.; Fortunelli, A.; Chen, C.-Y.; Yu, R.; Zhang, Q.; Gu, L.; Merinov, B.V.; Lin, Z.; et al. Ultrafine Jagged Platinum Nanowires Enable Ultrahigh Mass Activity for the Oxygen Reduction Reaction. *Science* **2016**, *354*, 1414–1419.
12. Burda, C.; Chen, X.; Narayanan, R.; El-Sayed, M.A. Chemistry and Properties of Nanocrystals of Different Shapes. *Chem. Rev.* **2005**, *105*, 1025–1102.
13. Jones, M.R.; Osberg, K.D.; Macfarlane, R.J.; Langille, M.R.; Mirkin, C.A. Templated Techniques for the Synthesis and Assembly of Plasmonic Nanostructures. *Chem. Rev.* **2011**, *111*, 3736–3827.
14. Wang, Y.; Black, K.C.L.; Luehmann, H.; Li, W.; Zhang, Y.; Cai, X.; Wan, D.; Liu, S.-Y.; Li, M.; Kim, P.; et al. Comparison Study of Gold Nanohexapods, Nanorods, and Nanocages for Photothermal Cancer Treatment. *ACS Nano* **2013**, *7*, 2068–2077.
15. Linic, S.; Christopher, P.; Ingram, D.B. Plasmonic-Metal Nanostructures for Efficient Conversion of Solar to Chemical Energy. *Nat. Mater.* **2011**, *10*, 911–921.
16. Lee, I.; Delbecq, F.; Morales, R.; Albitzer, M.A.; Zaera, F. Tuning Selectivity in Catalysis by Controlling Particle Shape. *Nat. Mater.* **2009**, *8*, 132–138.
17. Reske, R.; Mistry, H.; Behafarid, F.; Roldan Cuenya, B.; Strasser, P. Particle Size Effects in the Catalytic Electroreduction of CO₂ on Cu Nanoparticles. *J. Am. Chem. Soc.* **2014**, *136*, 6978–6986.
18. Singh, A.R.; Rohr, B.A.; Schwalbe, J.A.; Cargnello, M.; Chan, K.; Jaramillo, T.F.; Chorkendorff, I.; Nørskov, J.K. Electrochemical Ammonia Synthesis—The Selectivity Challenge. *ACS Catal.* **2017**, *7*, 706–709.
19. Kang, Y.; Li, M.; Cai, Y.; Cargnello, M.; Diaz, R.E.; Gordon, T.R.; Wieder, N.L.; Adzic, R.R.; Gorte, R.J.; Stach, E.A.; et al. Heterogeneous Catalysts Need Not Be so “Heterogeneous”: Monodisperse Pt Nanocrystals by Combining Shape-Controlled Synthesis and Purification by Colloidal Recrystallization. *J. Am. Chem. Soc.* **2013**, *135*, 2741–2747.
20. Kline, T.R.; Paxton, W.F.; Mallouk, T.E.; Sen, A. Catalytic Nanomotors: Remote-Controlled Autonomous Movement of Striped Metallic Nanorods. *Angew. Chem. Int. Ed.* **2005**, *44*, 744–746.

21. Choi, S.-I.; Xie, S.; Shao, M.; Odell, J.H.; Lu, N.; Peng, H.-C.; Protsailo, L.; Guerrero, S.; Park, J.; Xia, X.; et al. Synthesis and Characterization of 9 nm Pt–Ni Octahedra with a Record High Activity of 3.3 A/mg_{Pt} for the Oxygen Reduction Reaction. *Nano Lett.* **2013**, *13*, 3420–3425.
22. Zhang, J.; Yang, H.; Fang, J.; Zou, S. Synthesis and Oxygen Reduction Activity of Shape-Controlled Pt₃Ni Nanopolyhedra. *Nano Lett.* **2010**, *10*, 638–644.
23. Xie, M.; Shen, M.; Chen, R.; Xia, Y. Development of Highly-Active Catalysts toward Oxygen Reduction by Controlling the Shape and Composition of Pt–Ni Nanocrystals. *ACS Appl. Mater. Interfaces* **2023**, *15*, 49146–49153.
24. Xia, Y.; Gilroy, K.D.; Peng, H.-C.; Xia, X. Seed-Mediated Growth of Colloidal Metal Nanocrystals. *Angew. Chem. Int. Ed.* **2017**, *56*, 60–95.
25. Zhang, H.; Li, W.; Jin, M.; Zeng, J.; Yu, T.; Yang, D.; Xia, Y. Controlling the Morphology of Rhodium Nanocrystals by Manipulating the Growth Kinetics with a Syringe Pump. *Nano Lett.* **2011**, *11*, 898–903.
26. Peng, H.-C.; Park, J.; Zhang, L.; Xia, Y. Toward a Quantitative Understanding of Symmetry Reduction Involved in the Seed-Mediated Growth of Pd Nanocrystals. *J. Am. Chem. Soc.* **2015**, *137*, 6643–6652.
27. Wang, C.; Huang, Z.; Ding, Y.; Xie, M.; Chi, M.; Xia, Y. Facet-Controlled Synthesis of Platinum-Group-Metal Quaternary Alloys: The Case of Nanocubes and {100} Facets. *J. Am. Chem. Soc.* **2023**, *145*, 2553–2560.
28. Wang, C.; He, J.; Xia, Y. Controlling the Composition and Elemental Distribution of Bi- and Multi-Metallic Nanocrystals via Dropwise Addition. *Nat. Synth.* **2024**, *3*, 1076–1082.
29. Niu, G.; Ruditskiy, A.; Vara, M.; Xia, Y. Toward Continuous and Scalable Production of Colloidal Nanocrystals by Switching from Batch to Droplet Reactors. *Chem. Soc. Rev.* **2015**, *44*, 5806–5820.
30. Zhou, M.; Wang, H.; Vara, M.; Hood, Z.D.; Luo, M.; Yang, T.-H.; Bao, S.; Chi, M.; Xiao, P.; Zhang, Y.; et al. Quantitative Analysis of the Reduction Kinetics Responsible for the One-Pot Synthesis of Pd–Pt Bimetallic Nanocrystals with Different Structures. *J. Am. Chem. Soc.* **2016**, *138*, 12263–12270.
31. Luty-Błocho, M.; Paclawski, K.; Wojnicki, M.; Fitzner, K. The Kinetics of Redox Reaction of Gold(III) Chloride Complex Ions with L-Ascorbic Acid. *Inorg. Chim. Acta* **2013**, *395*, 189–196.
32. Corbett, J.F. Pseudo First-Order Kinetics. *J. Chem. Educ.* **1972**, *49*, 663.
33. Yang, T.-H.; Gilroy, K.D.; Xia, Y. Reduction Rate as a Quantitative Knob for Achieving Deterministic Synthesis of Colloidal Metal Nanocrystals. *Chem. Sci.* **2017**, *8*, 6730–6749.
34. Smith, J.H.; Luo, Q.; Millheim, S.L.; Millstone, J.E. Decoupling Intrinsic Metal Ion Reduction Rates from Structural Outcomes in Multimetallic Nanoparticles. *J. Am. Chem. Soc.* **2024**, *146*, 34822–34832.
35. Rodrigues, T.S.; Zhao, M.; Yang, T.-H.; Gilroy, K.D.; da Silva, A.G.M.; Camargo, P.H.C.; Xia, Y. Synthesis of Colloidal Metal Nanocrystals: A Comprehensive Review on the Reductants. *Chem. Eur. J.* **2018**, *24*, 16944–16963.
36. Zhang, H.; Lu, Y.; Liu, H.; Fang, J. Controllable Synthesis of Three-Dimensional Branched Gold Nanocrystals Assisted by Cationic Surfactant Poly(Diallyldimethylammonium) Chloride in Acidic Aqueous Solution. *RSC Adv.* **2014**, *4*, 36757–36764.
37. Lee, H.; Habas, S.E.; Somorjai, G.A.; Yang, P. Localized Pd Overgrowth on Cubic Pt Nanocrystals for Enhanced Electrocatalytic Oxidation of Formic Acid. *J. Am. Chem. Soc.* **2008**, *130*, 5406–5407.
38. Wilkins, P.C.; Johnson, M.D.; Holder, A.A.; Crans, D.C. Reduction of Vanadium(V) by L-Ascorbic Acid at Low and Neutral pH: Kinetic, Mechanistic, and Spectroscopic Characterization. *Inorg. Chem.* **2006**, *45*, 1471–1479.
39. Yu, H.; He, J.; Li, K.K.; Huang, Q.; Ding, Y.; Xia, Y. Synthesis of Ag@Pd Nanocubes and Pd-Based Nanoframes via One-Shot Injection of a Halide-Free Precursor for Continuous Production in a Flow Reactor. *Chem. Eur. J.* **2025**, *31*, e202500201.
40. Fiévet, F.; Ammar-Merah, S.; Brayner, R.; Chau, F.; Giraud, M.; Mammeri, F.; Peron, J.; Piquemal, J.-Y.; Sicard, L.; Viau, G. The Polyol Process: A Unique Method for Easy Access to Metal Nanoparticles with Tailored Sizes, Shapes and Compositions. *Chem. Soc. Rev.* **2018**, *47*, 5187–5233.
41. Sun, Y.; Xia, Y. Shape-Controlled Synthesis of gold and silver nanoparticles. *Science* **2002**, *298*, 2176–2179.
42. Zhang, D.; Chen, Y.; Huang, Y.-S.; Huang, Q.; Kwan Li, K.; Xia, Y. Robust, Reproducible, and Scalable Synthesis of Silver Nanocubes. *Chem. Eur. J.* **2024**, *30*, e202400833.
43. Wiley, B.J.; Xiong, Y.; Li, Z.-Y.; Yin, Y.; Xia, Y. Right Bipyramids of Silver: A New Shape Derived from Single Twinned Seeds. *Nano Lett.* **2006**, *6*, 765–768.
44. Wiley, B.J.; Sun, Y.; Xia, Y. Synthesis of Silver Nanostructures with Controlled Shapes and Properties. *Acc. Chem. Res.* **2007**, *40*, 1067–1076.
45. Skrabalak, S.E.; Wiley, B.J.; Kim, M.; Formo, E.V.; Xia, Y. On the Polyol Synthesis of Silver Nanostructures: Glycolaldehyde as a Reducing Agent. *Nano Lett.* **2008**, *8*, 2077–2081.
46. Sun, Y.; Gates, B.; Mayers, B.; Xia, Y. Crystalline Silver Nanowires by Soft Solution Processing. *Nano Lett.* **2002**, *2*, 165–168.

47. Sun, Y.; Mayers, B.; Herricks, T.; Xia, Y. Polyol Synthesis of Uniform Silver Nanowires: A Plausible Growth Mechanism and the Supporting Evidence. *Nano Lett.* **2003**, *3*, 955–960.
48. Korte, K.E.; Skrabalak, S.E.; Xia, Y. Rapid Synthesis of Silver Nanowires through a CuCl- or CuCl₂-Mediated Polyol Process. *J. Mater. Chem.* **2008**, *18*, 437–441.
49. Chan, J.M.; Zhang, L.; Yuet, K.P.; Liao, G.; Rhee, J.-W.; Langer, R.; Farokhzad, O.C. PLGA–Lecithin–PEG Core–Shell Nanoparticles for Controlled Drug Delivery. *Biomaterials* **2009**, *30*, 1627–1634.
50. Fredenberg, S.; Wahlgren, M.; Reslow, M.; Axelsson, A. The Mechanisms of Drug Release in Poly(Lactic-Co-Glycolic Acid)-Based Drug Delivery Systems—A Review. *Int. J. Pharm.* **2011**, *415*, 34–52.